



# Rhizosphere microbiome functional diversity and pathogen invasion resistance build up during plant development

Jie Hu,<sup>1,2</sup> Zhong Wei <sup>1\*</sup>, George A. Kowalchuk,<sup>2</sup> Yangchun Xu,<sup>1</sup> Qirong Shen <sup>1</sup> and Alexandre Jousset<sup>1,2</sup>

<sup>1</sup>Jiangsu Provincial Key Lab for Organic Solid Waste Utilization, Key Lab of Plant Immunity, Jiangsu Collaborative Innovation Center for Solid Organic Waste Resource Utilization, National Engineering Research Center for Organic-based Fertilizers, Nanjing Agricultural University, Weigang 1, Nanjing, 210095, People's Republic of China.

<sup>2</sup>Institute for Environmental Biology, Ecology and Biodiversity, Utrecht University, Padualaan 8, 3584CH Utrecht, The Netherlands.

## Summary

**The rhizosphere microbiome is essential for plant growth and health, and numerous studies have attempted to link microbiome functionality to species and trait composition. However, to date little is known about the actual ecological processes shaping community composition, complicating attempts to steer microbiome functionality. Here, we assess the development of microbial life history and community-level species interaction patterns that emerge during plant development. We use microbial phenotyping to experimentally test the development of niche complementarity and life history traits linked to microbiome performance. We show that the rhizosphere microbiome assembles from pioneer assemblages of species with random resource overlap into high-density, functionally complementary climax communities at later stages. During plant growth, fast-growing species were further replaced by antagonistic and stress-tolerant ones. Using synthetic consortia isolated from different plant growth stages, we demonstrate that the high functional diversity of 'climax' microbiomes leads to a better resistance to bacterial pathogen invasion. By demonstrating that different life-history strategies**

**prevail at different plant growth stages and that community-level processes may supersede the importance of single species, we provide a new toolbox to understand microbiome assembly and steer its functionality at a community level.**

## Introduction

Plant roots are intimately associated with the rhizosphere microbiome, a specific microbial community that plays a key role in plant growth and health (Mendes *et al.*, 2011). Several root-associated microorganisms can positively influence plant growth (Lugtenberg and Kamilova, 2009). In ideal cases, these organisms assemble literally into a protective shield around the roots, resisting the invasion by soil-borne pathogens via competition for resources or production of antimicrobial compounds (Haas and Défago, 2005; Wei *et al.*, 2015). Unfortunately, this ideal case is more the exception than the norm, and microbiomes often do not efficiently protect plants. Understanding the parameters that lead to the microbiome's ability to keep plants healthy is essential to restore this functionality. Traditionally, most research on plant-associated microorganisms has focused on cataloguing individual traits linked to plant health (Lugtenberg and Kamilova, 2009). However, it remains challenging to extrapolate these mechanisms in a community context. Numerous studies have expressed microbiome functionality as a function of the presence of specific traits or species and relating those to environmental factors (Jeraldo *et al.*, 2012; Mendes *et al.*, 2014; Beckers *et al.*, 2017). However, recent studies have revealed that microbiome functionality, especially resistance to pathogen invasion, may emerge out of the interplay between species rather than the presence of a specific trait or species (Wei *et al.*, 2015; Saleem *et al.*, 2019). This shift from a 'resistance gene' to a 'community-level' perspective has the potential to deeply impact our ability to understand and guide microbiome assembly. In contrast to individual genes whose abundance is difficult to extrapolate beyond case studies, the buildup of community-level processes such as functional diversity (FD) is well documented and can be easily connected to

Received 2 March, 2020; revised 18 May, 2020; accepted 23 May, 2020. \*For correspondence. E-mail weizhong@njau.edu.cn; Fax. 86 25 84396260; Tel. +86 25 84396824.

a hypothesis-driven approach developed in community ecology (Fargione and Tilman, 2005). Community ecology concepts are slowly making their way into microbiome science, as illustrated by inference models predicting assembly processes as a function of phylogenetic relationships between co-occurring species (Stegen *et al.*, 2012; Dini-Andreote *et al.*, 2015) or the topology of species co-variation patterns (Shi *et al.*, 2016). These models however rely on a largely untested set of assumptions.

We use rhizosphere microbiome maturation during plant growth as a model system, addressing in particular changes in species life-history strategies and ecological interactions between co-occurring microorganisms as indicators of ongoing processes. Variation in rhizosphere microbiome composition across different plant growth stages is well acknowledged but hard to explain beyond correlations (Lundberg *et al.*, 2012; Chaparro *et al.*, 2014). We propose here to approach species turnover and changes in microbiome function using a niche-driven ecological succession model. Our major premise is that most ecosystems, including the rhizosphere environment, are dynamic and undergo succession, as illustrated for instance by the succession from pioneer to climax-associated populations in soils exposed in retreating glaciers (Tilman, 1987; Whittaker, 1993). During an ecological succession, each stage is linked with specific associated traits in the dominant species, placing current community composition in the light of a dynamic temporal process. Ecological succession is a major concept in community ecology and may, when applied to the rhizosphere microbiome, provide a new predictive framework for species and trait occurrence, explain how a suppressive microbiome assembles and provide new entry points to engineer its ability to prevent diseases.

Upon germination, plant roots can be seen as a pioneer ecosystem. They are virtually sterile, with the exception of a few endophytes. They will rapidly be colonized by the first wave of pioneer soil microorganisms (Dang and Lovell, 2000). Due to the low competition prevailing in pioneer ecosystems, we expect these early colonizers to be predominantly r-strategists, investing resources into a fast growth rate, at the cost of an inefficient resource use and a limited ability to withstand stress. Over time, as the rhizosphere matures, more microbial species reach the roots, and we expect the early colonizers to be replaced by slower-growing K-strategists able to use resources more thoroughly, better resist biotic stress caused by competitors and invest more resources into competitor inhibition (Pickett and McDonnell, 1989). Furthermore, we expect that competitive interactions will become more structured over time. While in young roots community composition may mainly be driven by stochastic factors, the tougher competition expected in later stages implies that species occupying closely related

niches are likely to be mutually exclusive (Helsen *et al.*, 2016). Therefore, we expect that resource use patterns of co-occurring species will be largely overlapping on young roots but will become more structured and complementary in mature communities. This together will lead to a higher FD of the whole microbiome at later growth stages (Díaz *et al.*, 2006). Ecological succession may also drive the invasibility of rhizosphere communities. High FD and toxicity have been consistently reported to constrain invasion (Jousset *et al.*, 2011b; Wei *et al.*, 2015; Hu *et al.*, 2016). As these two characteristics should be selected in climax ecosystems, communities sampled from older root systems may be more resistant to pathogen invasion.

In order to assess the importance of ecological succession as a blueprint for microbiome assembly and functionality, we combined a culture-independent, DNA-based census approach with the phenotypic characterization of representative isolates. We tracked community structure and phenotypic characteristics of microbial communities colonizing tomato roots in a non-sterile soil, throughout the full course of plant development from germination to fruiting. We expected that (i) bacterial density will increase during the maturation of the rhizosphere ecosystem, (ii) fast-growing ruderal species will be replaced by more stress-tolerant climax species, (iii) niche complementarity between co-occurring species will increase during rhizosphere maturation and (iv) communities from old root systems will be more resistant to pathogen invasion than those retrieved from young seedlings.

## Results

### *Dynamics of bacterial community density, diversity and structure*

Total bacterial density increased with time. While bacterial density in the seedling stage rhizosphere was slightly higher than in bulk soil, it increased 10-fold by the fruiting stage ( $F_{3,8} = 85.73$ ,  $p < 0.0001$ , Fig. 1A). Bacterial diversity on roots was in general lower than in the bulk soil ( $F_{3,8} = 4.38$ ,  $p = 0.0457$ , Fig. 1B). The rhizosphere microbial community structure of bulk soil was distinct from that of rhizosphere soil at all growth stages (seedling, flowering and fruiting;  $F_{3,8} = 2.29$ ,  $p = 0.002$ , Fig. 1C). On the other hand, the microbial community of flowering-stage rhizosphere microbiome was very similar to the fruiting-stage rhizosphere microbiome (Fig. 1C). Together, our results show that the rhizosphere microbial community abundance, diversity and structure were strongly influenced by plant development.

The relative abundance of the 10 most abundant rhizosphere bacterial phyla differed significantly between bulk soil and rhizosphere soil (Fig. 1D). In general, Proteobacteria,

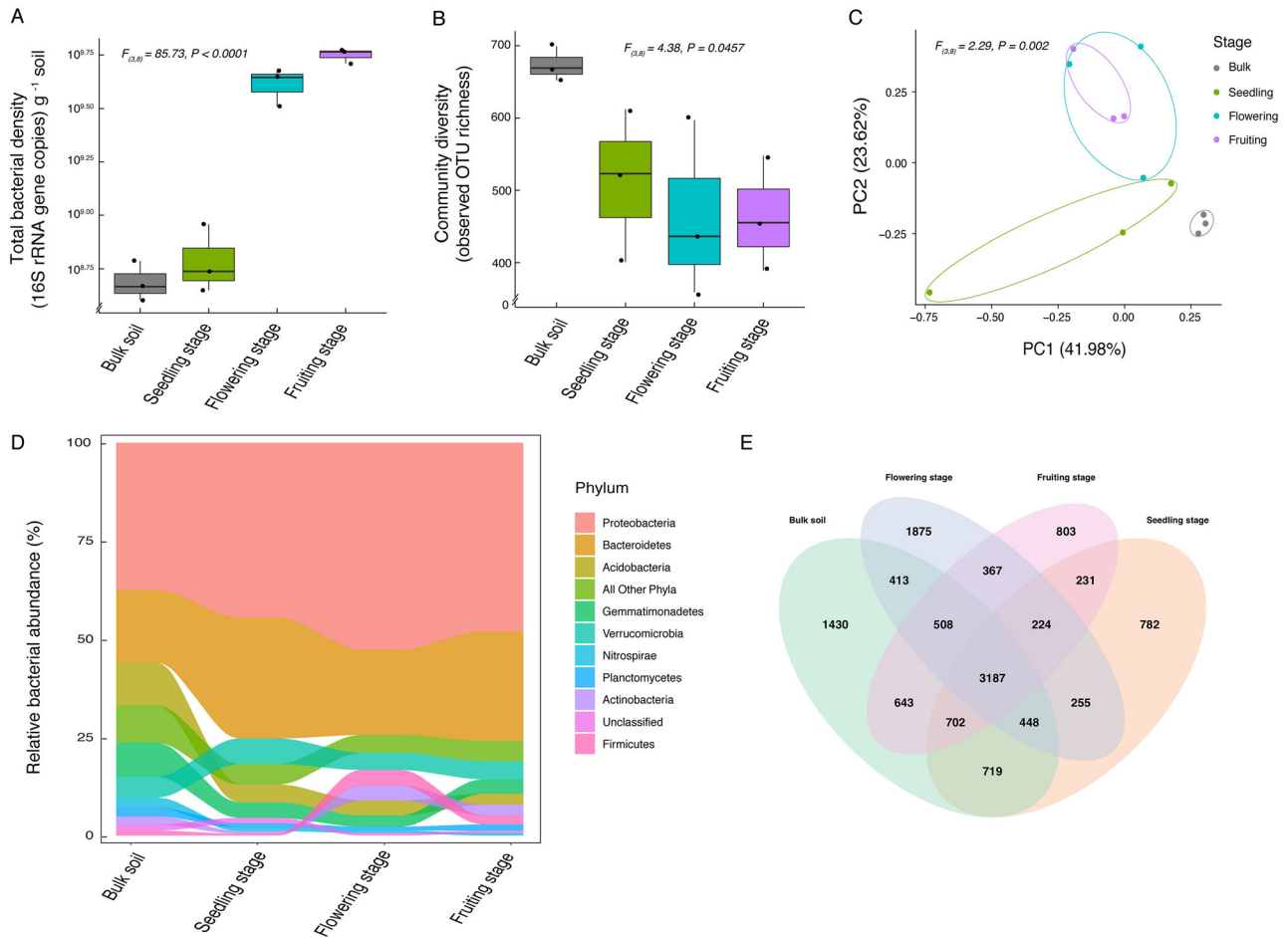


**Fig. 1.** Dynamics of soil and rhizosphere bacterial community composition at different tomato growth stages, as measured with cultivation-independent DNA metabarcoding. Panel A: 16S rRNA gene abundance per gram of rhizosphere soil as determined by qPCR. Panel B: Metabarcoding-inferred microbiome diversity, measured as the richness of observed OTUs with more than 10 reads per sample. Panel C: Community structure visualized by principal component analysis (PCA). Panel D: Changes in the relative abundance of the main bacterial during plant development. Each phylum is shown in a different color. Panel E: A Venn diagram displaying the number of unique and shared OTUs between plant development stages. [Color figure can be viewed at [wileyonlinelibrary.com](http://wileyonlinelibrary.com)]

Bacteroidetes and Acidobacteria are the most abundant bacterial phyla in both bulk soil and rhizosphere microbiome (Fig. 1D). Their relative abundance further varied with time, with for instance relative abundance of Bacteroidetes is higher in seedling stage microbiome compared with the bulk soil microbiome, while the relative abundance of Acidobacteria is higher in the bulk soil microbiome than in rhizosphere microbiome (Fig. 1D). The relative abundance of Firmicutes in the rhizosphere was highest at the flowering stage (Fig. 1D). No changes were observed in the relative abundance of other bacterial phyla among bulk soil and rhizosphere, regardless of the plant development stage (Fig. 1D).

Microbiomes from bulk soil and each different plant growth stage shared 3187 operational taxonomic units (OTUs) (Fig. 1E). More unique OTUs (1875) were recovered from the flowering-stage rhizosphere, a number that exceeded the unique OTUs found in bulk soil (1430). The

seedling-stage rhizosphere shared the most OTUs (719) with bulk soil compared with the flowering and fruiting stages (Fig. 1E).

#### Characterization of the cultivated bacterial isolates

We isolated bacteria from the rhizosphere of tomato plants at different growth stages and characterized a total of 331 isolates, corresponding to around 90 bacterial strains per growth stage. Bacterial isolates belonged to four different phyla (Proteobacteria, Firmicutes, Bacteroidetes and Actinobacteria), reflecting the abundance of these phyla in the soil and rhizosphere environment (Fig. 2A and B). Proteobacteria was the most represented phylum in our culture collection, with 52.3% of all isolates, followed by Firmicutes, Actinobacteria and Bacteroidetes with 35.6%, 8.2% and 3.6% of the isolates respectively. The isolated bacteria were affiliated to 35 different genera

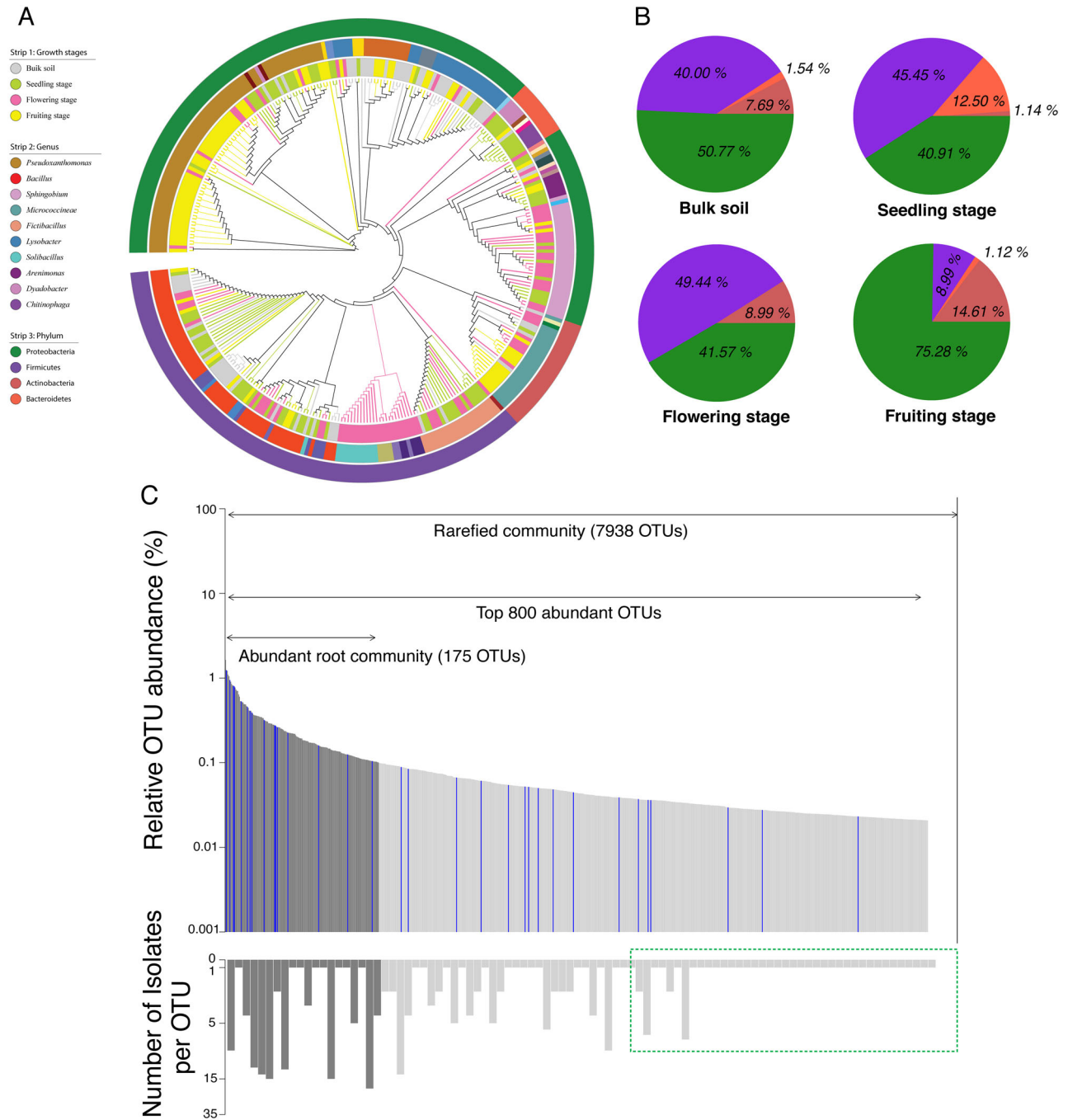


**Fig. 2.** Taxonomic and functional diversity of cultivable bacteria isolated from bulk soil and tomato rhizosphere soil at different plant growth stages. Panel A: Phylogenetic tree of all the isolates. The first strip indicates the plant growth stage from which isolates were retrieved, the second strip indicates the genus-level affiliation of each isolate (the 10 most abundant genera are shown, see Table S1 for a detailed list of all genera). The third strip indicates the phylum-level affiliation of all isolates. Panel B: Summary of the phylum-level taxonomic affiliations of all isolates at each growth stage, as determined by 16S rRNA gene sequence. Panel C: Matching of the bacterial isolates with 16S rRNA gene metabarcoding data. The upper bar graph represents the relative abundance of the 7938 OTUs retrieved across all samples, the 800 most abundant OTUs are highlighted in dark gray (relative abundance >0.1%). Blue bars denote OTUs that could be matched to at least one cultivated isolate. The lower, inverted bar graph indicates the number of isolated bacteria matching a given OTU. Bars inside the green dashed rectangle highlight isolates that matched to rare OTUs. [Color figure can be viewed at [wileyonlinelibrary.com](http://wileyonlinelibrary.com)]

(Fig. 2A; Table S1). We found three genera *Micrococcineae* (25), *Streptomycineae* (1) and *Corynebacterineae* (1) in the phylum Actinobacteria (27 isolates). In the phylum

Bacteroidetes (13 isolates), we noted five genera with *Chitinophaga* (5) and *Dyadobacter* (5) having more than one representative isolate. Among Firmicutes (118 isolates),

the genera *Bacillus* (59), *Fictibacillus* (22), *Solibacillus* (12) *Falsibacillus* (9) and *Lysinibacillus* (5) were the most abundant ones. In the most abundant phylum Proteobacteria (173), 19 genera were found, in which abundant *Pseudoxanthomonas* (71), *Lysobacter* (29) and *Sphingobium* (31) were included. The bacteria isolated from flowering-stage and fruiting-stage rhizospheres were more clustered to the bacteria isolated from the same growth stage, while bacteria isolated from bulk soil and seedling-stage rhizosphere were more distributed in different branches of the phylogenetic tree (Fig. 2A). The proportion of Proteobacteria and Actinobacteria recovered from the rhizosphere increased during plant development, while Bacteroidetes were of greatest relative abundance in the early stage of plant growth (Fig. 2B).

Overall, out of the 331 bacterial isolates, 298 (90.0%) matched 60 of the OTUs observed by Illumina sequencing (Fig. 2C), only 33 (10.0%) isolates could not be matched with a representative rhizosphere microbiome sequence. The matched OTUs covered both abundant and rare species. Our strain collection thus contained numerous strains that could be grouped into a single OTU as discriminated by the relatively short 16S rRNA gene fragments examined. All of the matched 60 OTUs were present in the rhizosphere microbiome (7938 OTUs) (Fig. 2C). The top 175 abundant OTUs all had a relative abundance higher than 0.1% across all sampled rhizosphere microbiomes. We were able to isolate 193 bacterial strains from 20 OTUs out of these top abundant 175 OTUs (Fig. 2C).

#### Functional diversity of cultivable bacteria

All bacteria could grow on one or more of the tested representative rhizosphere carbon sources. Generally, carbohydrates were used by more isolates (Fig. S1). As determined by resource use patterns of isolates collected from the same plant, functional diversity (FD) of cultivable bacterial communities increased during plant development, from a low FD in bulk soil and seedlings to the highest FD at the flowering stage, before slightly decreasing at the fruiting stage ( $F_{3,8} = 7.72$ ,  $p = 0.0095$ , Fig. 3A).

#### Bacterial stress tolerance

Abiotic stress tolerance was higher for bacteria isolated from the flowering and/or fruiting stages of plant growth as compared with the bulk soil and the seedling stage. Bacteria isolated from fruiting-stage rhizosphere samples were best at coping with low nutrient availability ( $F_{3,380} = 57.13$ ,  $p < 0.0001$ , Fig. 3B), while bacteria isolated from flowering-stage rhizosphere samples contained the highest oxidative and salinity stress tolerance

( $F_{3,380} = 21.7$ ,  $p < 0.0010$ , Fig. 3C and  $F_{3,380} = 4.70$ ,  $p = 0.0031$ , Fig. 3D). The coefficient of variation of nutrient limitation tolerance, an indicator for the co-occurrence of tolerant and susceptible isolates on a given plant, was significantly lower for the fruiting-stage rhizosphere as compared with other growth stages ( $F_{3,8} = 3.36$ ,  $p = 0.0409$ , Fig. S2A), indicating that isolates from the fruiting-stage rhizosphere microbiome shared a similar stress tolerance. The coefficients of variation for bacterial growth under oxidative or salinity stress did not vary across the growth stages (Fig. S2B, Fig. S2C).

#### Antagonistic activity against *Ralstonia solanacearum*

All bacteria isolated from the rhizosphere, and most of the ones isolated from bulk soil, showed some level of antagonism against the soil-borne bacterial pathogen *R. solanacearum*. The average toxicity increased with the growth stage, with the highest levels at the fruiting stage ( $F_{3,380} = 14.91$ ,  $p < 0.0001$ , Fig. 4A). In general, Gammaproteobacteria showed the highest level of antagonism, especially the bacteria isolated from the fruiting-stage rhizosphere (Fig. S3), and unclassified bacteria had the lowest antagonistic activity, except for flowering-stage isolates (Fig. S3). At the seedling stage, Cytophagia had the lowest level inhibition ability to the pathogen (Fig. S3). A high level of variation was observed with respect to the antagonistic activities of the screened isolates. This heterogeneity was most pronounced in the bulk soil, was more modest at the seedling growth stage and increased further with subsequent plant development ( $F_{3,8} = 8.71$ ,  $p = 0.0067$ , Fig. 4B). The higher levels of variation in bulk soil isolates may be explained by the heterogeneity of soil or the absence of a selective pressure for or against antagonism. The increase in the coefficient of variation of different traits with plant age suggests that young plants may have conditions favoring ruderal species investing comparatively little energy into the production of toxic secondary metabolites, while at later stages various life-history strategies may coexist.

#### Microbiome invasion resistance against *R. solanacearum*

In order to test whether resource use and antagonism patterns were reflected in invasibility, we assessed the ability of consortia re-assembled out of the 32 isolates recovered from each plant to resist invasion by *R. solanacearum* in a co-culture experiment. All re-assembled consortia could suppress pathogen growth compared with the control, although the magnitude of this effect differed with respect to the growth stage from which consortia originated ( $F_{3,8} = 7.36$ ,  $p = 0.0109$ , Fig. 5). Pathogen

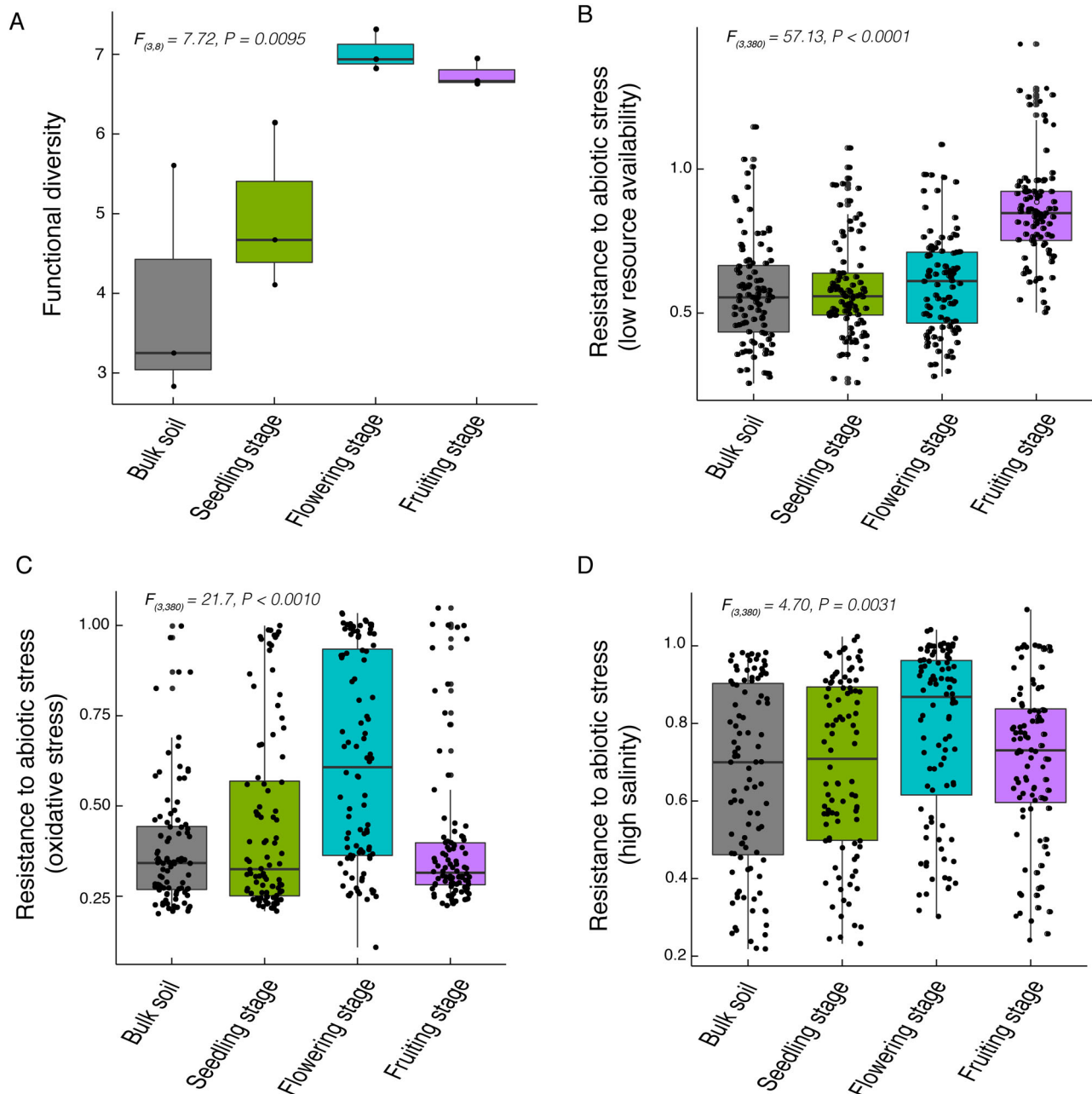


**Fig. 3.** Changes in the life history strategies of the isolated root-associated bacteria during tomato plant development. Panel A: Functional diversity (FD) of cultivable bacteria isolated at different plant growth stages. FD was defined on the base of resource use patterns of individual isolates on representative plant-derived carbon sources, calculated independently for each plant and time point (32 bacterial isolates per plant and time point). Panels B–D: Abiotic stress resistance of bacteria isolated from tomato roots at different growth stages. Stress resistance was defined as the relative growth of each isolate in the liquid medium. Three stressors were assessed: low resource availability (10× reduction in culture medium concentration), oxidative stress (1 mM  $H_2O_2$ ) or high salinity (200 mM NaCl). One point represents one isolate. [Color figure can be viewed at [wileyonlinelibrary.com](http://wileyonlinelibrary.com)]

suppression was highest for consortia reassembled out of bacteria isolated from the flowering-stage tomato rhizosphere.

Since communities from flowering and fruiting stages also displayed higher taxonomic diversity, FD, resistance to stress and toxicity against pathogen, we tested whether we could predict consortium suppressiveness on pathogen

based upon these four parameters. We found that the FD of each consortium, calculated on the base of the resource utilization, was the best predictor for level pathogen inhibition (Table 1). In contrast, taxonomic diversity, variability of stress resistance (another component of FD) and average inhibitory activity of the individual species were only poor predictors of pathogen inhibition (Table 1). This suggests

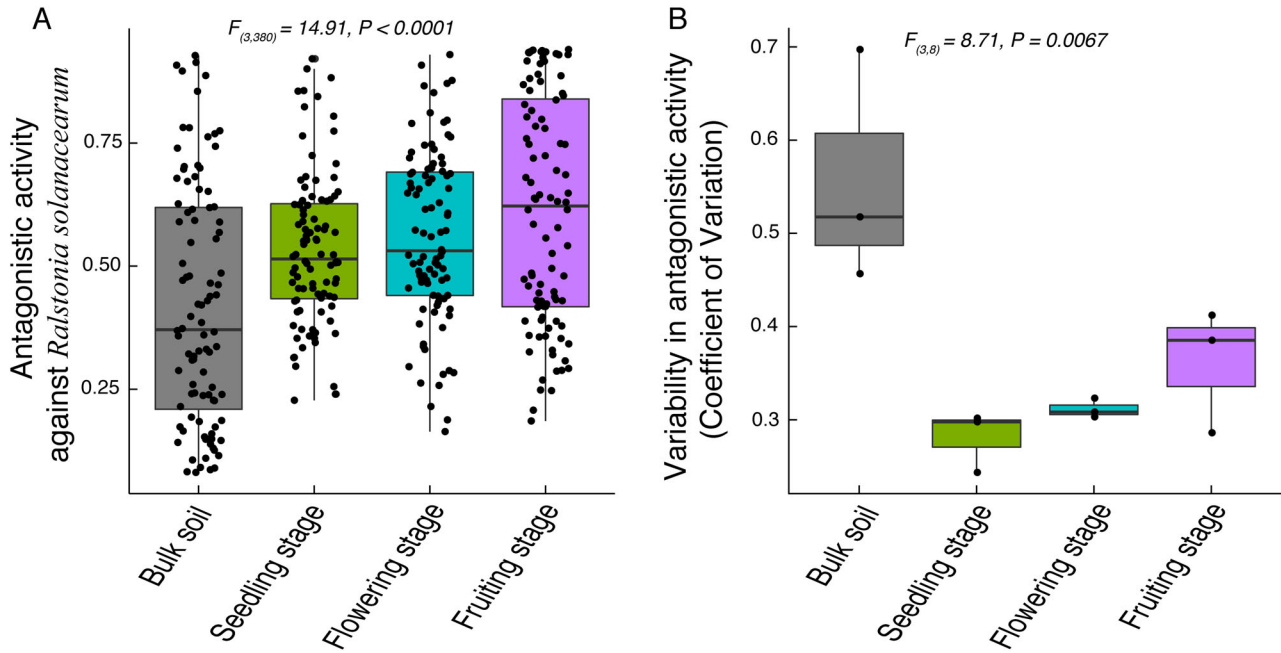


**Fig. 4.** Inhibitory activity of supernatants from bacteria isolated from tomato rhizosphere at different growth stages. Panel A: Supernatants were tested against the soil-borne bacterial pathogen *Ralstonia solanacearum* and inhibition defined as the reduction in pathogen growth compared with the control. Each point shows one bacterial isolate. Panel B: Coefficient of variation for each of the analysed samples. A high coefficient of variation (CV) indicates that different isolates co-occurring in one plant varied in their antagonistic activity, a low CV that all tested isolates from one plant shared the same strategy. Each point represents the coefficient of variation for one plant. [Color figure can be viewed at [wileyonlinelibrary.com](http://wileyonlinelibrary.com)]

that, in contrast to common assumptions, invasibility may be mainly driven by resource competition instead of antagonism.

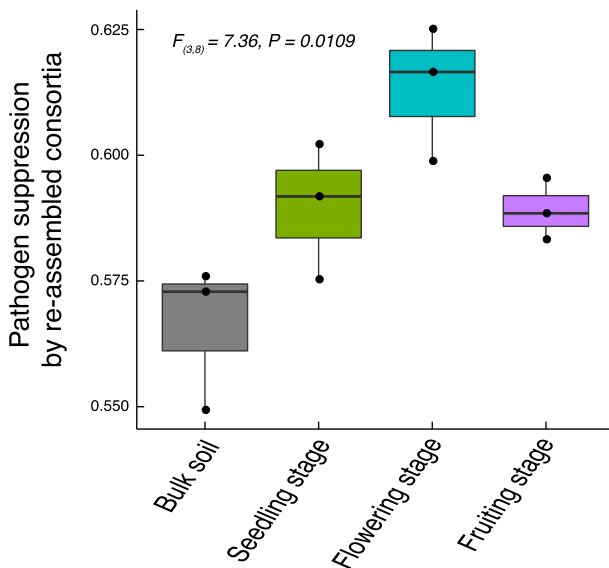


**Fig. 5.** Community-level pathogen suppression ability of re-assembled bacterial consortia. Consortia were re-assembled out of the 32 bacterial isolates isolated from each single plant sample and grown in liquid medium under invasion by the bacterial pathogen *Ralstonia solanacearum*. Pathogen suppression was defined as the reduction of pathogen density at the end of the experiment when the pathogen was co-cultured with the re-assembled consortia relative to its density when grown in isolation. Each point represents one re-assembled consortium. [Color figure can be viewed at [wileyonlinelibrary.com](http://wileyonlinelibrary.com)]

## Discussion

The rhizosphere microbiome is recognized as a major determinant of plant growth and health. Plant roots are colonized by a subfraction of bulk soil microbial species which, fed by plant-derived carbon, provide several services to the host plant (Marilley and Aragno, 1999; Molina, 2000; Morgan *et al.*, 2005). However, despite a

**Table 1.** ANOVA table expressing the resistance of re-assembled microbial consortia against invasion by the bacterial pathogen *Ralstonia solanacearum* as a function of taxonomic diversity, functional diversity, the stability of life-history strategies and average antagonistic activity.

Factors/function	Pathogen suppression		
	df	<i>p</i> -value	<i>F</i>
Taxonomic diversity	1	0.2491	1.58
Functional diversity	1	<b>0.0317</b>	<b>7.16</b>
Stability under stress	1	0.1163	3.21
Antagonistic competition ability	1	0.3682	0.93
Residuals	7		
Model summary	$R^2 = 0.45; AIC = -60.85$		

Taxonomic diversity is calculated based on bacterial identification at the genus level. Functional diversity was calculated based on the bacterial carbon source utilization ability. Stability under stress was defined as the average value of variation coefficient for bacterial community growth under three different stresses (reduced nutrient availability, oxidative stress and high salinity). Antagonistic competition ability was defined as pathogen suppression by bacterial supernatant. Significant results ( $p < 0.05$ ) are highlighted in bold.

highly detailed knowledge on which species are present around plant roots and which functional genes they carry, little is known about the factors driving species composition and microbiome function. Previous studies have highlighted that gut and rhizosphere microbiomes rapidly develop together with their host (Koenig *et al.*, 2011; Chaparro *et al.*, 2014). Some studies have sought to infer the contribution of niche versus stochastic processes based on species distribution data (Jeraldo *et al.*, 2012; Mendes *et al.*, 2014; Beckers *et al.*, 2017) and have revealed a widespread niche-driven microbiome assembly. However, to date, the exact underlying mechanisms have not been validated, with individual-level properties being only roughly inferable from sequence data. Furthermore, while the host-mediated filtering of microbial communities by root exudates is well recognized to be important (Smalla *et al.*, 2001), a temporal approach that addresses microbiome development in a dynamic context is still generally missing.

Here, by using a combination of DNA-based community mapping and isolate phenotyping we demonstrate that the rhizosphere microbiome undergoes a dynamic turnover following a classical ecological succession pattern. In particular, we show for the first time that real interactions change with time: resource competition between co-occurring organisms goes down as indicated by increased niche differentiation. While the average level of resource use by single microbes did not change significantly with time, the sorting of species across the available resource space became more pronounced, leading to a high FD of mature microbiomes. Different life-history strategies could coexist in older plants, potentially because older roots offer a wealth of different micro-niches that are preferentially colonized by different phenotypes (Achouak *et al.*, 2004). Finally, antagonistic interactions went up during plant development, as illustrated by the higher level of pathogen inhibition by isolates collected from plants in their flowering and fruiting stages.

These patterns indicate a shift from a random community assembly to a more niche-driven one over the course of plant growth. While the role of niche processes during community succession has been emphasized in previous studies (Stegen *et al.*, 2012), the present work is to our knowledge the first to demonstrate experimentally the presence of niche differentiation during microbiome maturation. The shifts in microbiome composition can be connected with the microbiome function. High FD is generally associated with a better community function (Cadotte *et al.*, 2011), and we indeed found that more functionally diverse communities from the later plants reached a density up to ten times higher than observed for communities comprised of overlapping species colonizing seedlings.

We propose on the basis of these results that the adaptation to the rhizosphere environment should be

approached from a community and not a purely species perspective. Instead of approaching the rhizosphere only as a filter selecting for species carrying specific traits (Barret *et al.*, 2011), we propose to shift the focus towards the selection for increasingly structured patterns of interactions between co-occurring species, including niche complementarity and antagonism, with microbiome function being selected as an emerging property of these interactions (Garcia and Kao-Kniffin, 2018; Li *et al.*, 2019). This selection for a functionally diverse community in the rhizosphere is illustrated both by the high niche complementarity and the high coexistence of different life-history strategies, covering the growth, stress resistance and antagonistic activity of co-occurring microorganisms, which increases during microbiome maturation. We explain this pattern both by ecological succession and by the increased complexification of the root system during plant development, with the resulting broader ecological niches likely favoring complementary interactions over antagonistic ones (Dimitrakopoulos and Schmid, 2004; Jousset *et al.*, 2011a). We propose that part of the ecological succession and species sorting may have been enabled by the complexity of the root system during plant growth. Further studies relating root morphology to microbiome composition are, however, necessary to unravel the links between microhabitat diversity and microbiome assembly and function (Pérez-Jaramillo *et al.*, 2018).

In contrast to the rapid niche differentiation occurring in terms of resource use patterns, the average production of antimicrobial compounds only gradually increased with plant development. We propose that this directional selection for more toxicity may have emerged as a consequence of competition. New roots represent a relatively open environment, colonized by a low density of microorganisms. Under these conditions, antagonizing competitors may be of only marginal value for fitness compared with the ability to grow fast (Kährström, 2014). In contrast, on more mature plants, where microbial density is high, conditions favor antagonism as a way to out-compete other species (Smead and Forber, 2013).

The community-level selection of functionally diverse species assemblages during microbiome maturation may have important consequences for microbiome function and plant health. Re-assembled consortia from bacteria isolated from mature plants were the most resistant against pathogen invasion, a pattern that we could link to the higher FD of the communities. These consortia are conceived as a simplified version representative of the interactions taking place in the rhizosphere microbiome. While we did not explicitly test invasion under natural rhizosphere conditions, previous studies have demonstrated that *in vitro* resource competition patterns can be used to infer plant protection levels (Wei *et al.*, 2015;



Li *et al.*, 2019). This study, therefore, contributes to the growing evidence that community-level trophic interactions may be more relevant to control pathogens than the presence of specific traits in one of the present bacteria. We should nonetheless keep in mind that rare and non-cultivable species, which may have been overlooked missed in this work, may also play an important role in microbiome function (Jousset *et al.*, 2017).

From an applied perspective, our results have various implications for our understanding of microbiome functioning. In particular, we shift the interpretation of disease suppressiveness from a single strain or trait (Weller *et al.*, 2002; Mendes *et al.*, 2011) to a community-level approach (Saleem *et al.*, 2019). For instance, the low FD on microorganisms associated with seedlings provides an explanation for the high vulnerability of early life microbiome to pathogen attack. We further suggest that, instead of searching and augmenting microorganisms harboring specific sets of traits such as antibiotics (Dinesh *et al.*, 2015), we might steer microbiome succession to favor functionally diverse assemblages that will outcompete pathogens. Previous studies have demonstrated that the interplay of co-occurring species, as opposed to the presence or absence of a given species or functional traits, is a major determinant of disease suppression (Wei *et al.*, 2015; Hu *et al.*, 2016; Li *et al.*, 2019). Active interventions aiming at speeding up the assembly of functionally diverse communities may help control early life diseases such as *Pythium* damping-off. Achieving such fast-forwarded microbiome assembly may be facilitated by either adding microbial species complementing the existing ones or by priming soil with resources that will pre-select microbial communities showing high resource complementarity while efficiently being able to colonize young plants.

In conclusion, we demonstrate a rapid turnover in life-history strategies during microbiome buildup over the course of plant development, a phenomenon that cannot be gleaned from the pure examination of DNA-based census approaches. We advocate that approaching the competitive and facilitative interactions between species may represent and oversee mechanism explaining microbial turnover and community maturation without the need to assume an active steering by the host plant.

## Experimental procedures

### *Experimental soils, plants and sampling process*

**Experimental soils.** Experiments were conducted using a non-sterile soil collected from Yixing, China (31.34 N 119.82 E). The soil is a sandy soil with the following physicochemical characteristics: pH 6.39; 28.69 g kg<sup>-1</sup> organic carbon; 79.41 mg kg<sup>-1</sup> available nitrogen content;

25.77 mg kg<sup>-1</sup> available phosphate and 59.44 mg kg<sup>-1</sup> available potassium. After removing surface debris (5 cm) on the ground, the soil was collected from a depth of 5–20 cm. All experimental soils were sieved (5 mm mesh size), homogenized and stored at 4°C until the subsequent pot experiment.

**Experimental plants.** Tomato seeds (*Lycopersicon esculentum*, cultivar ‘Jiangsu’) were sterilized by immersing in 0.5% NaOCl for 5 min and washing five times in sterile distilled water, and germinated on water-agar plates for 3 days at 28°C in the dark before sowing into seedling plates containing <sup>60</sup>Co-sterilized seedling substrate (Huainong, Huaian soil and fertilizer Institute, Huaian, China). Seedlings were transplanted at the three-leaf stage (12 days after sowing) into individual pots containing 5 kg homogenized experimental soil each. After transplantation, tomato plants were grown for up to 60 days in a greenhouse (temperature ranging from 25°C to 35°C) and watered two to three times per week. Pots containing tomato plants were randomly rearranged every 2 days.

**Soil sampling process.** We destructively sampled tomato plants at 0 (bulk soil), 5 (early vegetative or seedling stage), 35 (flowering stage) and 60 days (fruiting stage) after transplantation. Three plants were sampled at each growth stage. To harvest rhizosphere soil, we first gently removed the plants from the pots, shook off excess soil from the root system, and the soil attached to the root system was collected. One part of each sample was stored at 4°C for isolation of microorganisms, while the other part was stored at –80°C until subsequent DNA extraction.

### *DNA extraction, sequencing and bacterial density quantification*

We used the Power Soil DNA Isolation Kit (Mobio Laboratories, Carlsbad, CA, USA) to extract total soil DNA from 0.3 g of rhizosphere or bulk soil samples, following the manufacturer’s protocol. DNA concentration and purity were determined with NanoDrop 1000 spectrophotometer (Thermo Scientific, Waltham, MA, USA).

For PCR amplification, we used the 563F (5'-AYT GGG YDT AAA GVG-3') and 802R (5'-TAC NVG GGT ATC TAA TCC-3') (Cardenas *et al.*, 2010) primer pair, which targets the V4 hypervariable region of the bacterial 16S rRNA gene. The first round of PCR was used to attach the barcodes to primers for MiSeq sequencing (Shanghai BIOZERON Biotechnology). The second round of PCR was then used for paired-end sequencing using Y-shaped adapters. Amplicons were purified using magnetic beads denaturation using fresh NaOH (Bordelon *et al.*, 2013). The denatured amplicons were

sequenced using a chip-based bridge amplification procedure synthesizing one nucleotide per each cycle by using reversible terminator dye nucleotides (Voelkerding *et al.*, 2009).

After filtering, on average 45 678 high-quality sequences (min = 37 524 and max = 57 173) per sample were obtained and included for subsequent analyses. The OTU abundance of each sample was standardized by using the lowest level (37 524) of sequence depth as a reference. After discarding unqualified reads, the OTUs were assigned at 97% identity level using UPARSE (version 7.1) (Edgar, 2013). After the OTU assignment, a total of 16 867 OTUs were included in further analyses. The phylogenetic affiliation of each 16S rRNA gene sequence was analysed using the RDP Classifier (Margsin *et al.*, 2011) against the Silva 16S rRNA gene database with a confidence threshold of 70% (Amato *et al.*, 2013). Raw sequences were deposited into the NCBI Sequence Read Archive (SRA) database under the accession number PRJNA545482.

We used quantitative PCR (qPCR) to quantify the density of bacterial 16S rRNA gene copies per gram of soil. To this end, we used the primer pair Eub338: 5'-ACT CCT ACG GGA GGC AGC AG-3' and Eub518: 5'-ACT CCT ACG GGA GGC AGC AG-3' (Yarwood *et al.*, 2010). The qPCR analyses were carried out using the Applied Biosystems 7500 Real-Time PCR System (Applied Biosystems, CA, USA) via SYBR Green I fluorescent dye. Each reaction (20  $\mu$ l volume) contained 10  $\mu$ l of SYBR Premix Ex Taq (Takara Biotech, Japan), 2  $\mu$ l of DNA template and 0.4  $\mu$ l of both forward and reverse primers and 7.2  $\mu$ l of deionized water. PCR was performed by initially denaturing at 95°C for 30 s and cycling 40 times with a 5-s denaturing step at 95°C. This was followed by a 34-s elongation step at 60°C and melting curve was analysed at 95°C for 15 s, at 60°C for 1 min and at 95°C for 15 s.

#### *Bacterial isolation and identification*

We isolated bacteria from the bulk and rhizosphere soils as follows: One gram of soil was suspended in 9 ml of sterile distilled water, vortexed vigorously and subsequently serially diluted. Hundred microliters of the  $10^{-4}$ – $10^{-7}$  dilutions were plated onto 1/3 TSA agar plates (tryptone 5 g L<sup>-1</sup>, soy peptone 1.65 g L<sup>-1</sup>, NaCl 1.65 g L<sup>-1</sup> and agar 15 g L<sup>-1</sup>). Plates were incubated at 28°C for 5 days before we selected 32 single colonies from each root sample according to the bacterial morphology, isolations were always selected from the  $10^{-5}$  dilution. Bacterial colonies were purified by streaking on TSA agar plates and incubated overnight at 28°C. A total of 384 bacterial strains were isolated and stored at –80°C in 20% glycerol (vol/vol).

We identified the isolates on the base of their 16S rRNA gene sequence using the 16S rRNA universal primers 5'-AGA GTT TGA TCA TGG CTC AG-3' (F27) and 5'-TAC GGT TAC CTT GTT ACG ACT T-3' (R1492) (Heuer *et al.*, 1997). PCR reactions were carried out in 25  $\mu$ l volume by using 1  $\mu$ l of bacterial culture suspension, 12.5  $\mu$ l PCR reaction mixture, 1  $\mu$ l of forward and reverse primer each and 9.5  $\mu$ l of deionized water. Thermocycling was as follows: initial denaturation at 95°C for 5 min, 30 cycles of denaturation at 94°C for 30 s, annealing at 58°C for 30 s, extension at 72°C for 1 min 30 s and a final extension at 72°C for 10 min. PCR products were sequenced by Shanghai Sangon Biotechnology, Shanghai Station. 16S rRNA gene sequencing results were blasted against the NCBI database for homologous sequences. All sequences were deposited into the NCBI SRA database under the temporary accession number SUB5694723. Bacteria isolate sequences were aligned using the PyNAST algorithm in QIIME v 1.8. The phylogenetic tree file was generated using FastTree imported into iTOL: Interactive Tree Of Life, and visualization was conducted in iTOL.

#### *Matching bacterial isolates with OTUs*

To cross-reference cultivation-independent and dependent methods, we mapped the 16S rRNA sequences of the bacterial isolates in the tomato rhizosphere to the OTU representative sequences obtained from the microbiome sequence data of V4 hypervariable region of the bacterial 16S rRNA gene. The quality-filtered, full-length sequences of the isolates were trimmed 5' of the 799F primer site using FLEXBAR v2.4 and trimmed to 360 bp to identify the same region of the 16S rRNA operon as used for microbiome sequence. The trimmed isolate sequences were then mapped to the OTU representative sequences at  $\geq 97\%$  sequence similarity using UPARSE (Edgar, 2013).

#### *Carbon resource utilization patterns of the bacterial isolates*

We assessed the resource use patterns of all 384 bacterial isolates on 37 different single carbon resources (Table S2) representative of tomato root exudates (Wei *et al.*, 2015). Briefly, overnight tryptic soy broth cultures of bacterial isolates (TSB, tryptone 15 g L<sup>-1</sup>, soy peptone 5 g L<sup>-1</sup> and NaCl 5 g L<sup>-1</sup>) were pelleted by centrifugation (4000g, 3 min), washed three times in 0.85% NaCl and adjusted to an OD<sub>600</sub> of 0.5. Bacterial growth in each substrate was determined in 96-well microtiter plates containing 150  $\mu$ l OS minimal medium (Schnider-Keel *et al.*, 2000) supplemented with 10 mM of single resources representative of amino acids, organic acids and sugars

found in tomato root exudates (Wei *et al.*, 2015). The list of the 37 substrates used in this analysis is given in Table S2.

Bacteria were added to 96-well microtiter plates with an initial bacterial density of OD<sub>600</sub> of 0.05, after which plates were incubated for 24 h at 30°C with agitation (170 rpm). The plate layout was randomized to avoid biases due to evaporation differences according the distance to the plate edge. After incubation, bacterial growth density was estimated as the OD<sub>600</sub>, recorded with a Spectra Max M5 spectrophotometer (Molecular Devices, Sunnyvale, CA, USA). Community-level resource utilization ability was characterized using FD based on quantitative substrate utilization metrics (see statistics below for the calculation method description).

#### *Abiotic stress resistance test of the bacterial isolates*

We assessed the growth ability of each individual strain under limited resource availability, oxidative stress and high salinity stress as indicators of their potential to cope with sub-optimal growth conditions. We cultured all bacteria in 96-well microplates (initial density of OD<sub>600</sub> of 0.05) either in full TSB medium or with abiotic stressors (10% TSB medium as limited nutrient availability, full TSB medium with 1 mM H<sub>2</sub>O<sub>2</sub> as oxidative stress and full TSB medium with 200 mM NaCl as high salinity stress) for 24 h at 30°C with shaking (170 rpm). After 24 h incubation, bacterial density was recorded with a spectrophotometer at the optical length at 600 nm (Spectra Max M5, Molecular Devices). Bacterial tolerance to abiotic stressors was defined as the ratio of bacterial density under different stressors and full TSB medium.

#### *Production of antagonistic secondary metabolites*

We estimated the antibacterial activity of the different isolates by testing the inhibitory potential of their cell-free supernatants against *Ralstonia solanacearum* QL-Rs1115 (Wei *et al.*, 2011), a widespread soil-borne plant pathogenic bacterium causing damage to more than 200 crops including tomato (Jiang *et al.*, 2017). We cultured all the bacterial strains individually in TSB for 30 h (30°C, 170 rpm), after which cells were pelleted by centrifugation (4000g, 3 min) and supernatants were sterile filtered (0.22 µm). Cell-free supernatants were then used immediately for pathogen inhibition experiments. Briefly, 20 µl of supernatant was added to 180 µl fresh Casamino acid–Peptone–Glucose (CPG) medium (Casamino acid 1 g L<sup>-1</sup>, Peptone 10 g L<sup>-1</sup> and Peptone 5 g L<sup>-1</sup>) containing the pathogen *R. solanacearum* with an initial OD<sub>600</sub> of 0.05. Control treatments received 20 µl CPG media instead of bacterial supernatants. *Ralstonia solanacearum* was grown for 24 h (30°C, 170 rpm), and

pathogen density was evaluated on the base of the value of OD<sub>600</sub> using a Spectra (Max M5 Plate reader, Molecular Devices). The antagonistic activity of each bacterium was defined as the relative pathogen growth reduction in the presence of its supernatant compared with the control treatment.

#### *Pathogen invasion resistance of re-assembled consortia*

In order to assess whether microbiome assembly affected pathogen invasion resistance at a community level, we re-assembled synthetic consortia out of the 32 bacteria isolated from each plant and subjected them to invasion by *Ralstonia solanacearum*, see Table S3 for more details about bacterial composition in each re-assembled synthetic consortium. All isolated bacterial strains were grown overnight, washed in 0.85% NaCl and adjusted to an OD<sub>600</sub> of 0.5. The 32 bacterial strains from the same individual plant were then mixed together at equal initial biomass, resulting in 12 distinct re-assembled consortia. Two microliters of each re-assembled consortium and 0.5 µl of mCherry-tagged *Ralstonia solanacearum* (Wei *et al.*, 2015) (both at an OD<sub>600</sub> of 0.5) were inoculated into 180 µl CPG medium in 96-well microplates and grown for 24 h (30°C, 170 rpm). Three technical replicates were set up for each treatment. After 24 h, we measured total bacterial density as the OD<sub>600</sub> and pathogen growth as the mCherry signal (excitation wavelength of 587 nm, emission wavelength of 610 nm) with a Spectra Max M5 Plate reader (Molecular Devices), as previously described (Wei *et al.*, 2015). Both OD<sub>600</sub> and mCherry signals were blanked against the signal of the sterile CPG medium. As a reference, the pathogen was grown in isolation. Invasion resistance was defined as the percentage of reduction in pathogen growth compared with pathogen growth in the reference control treatment.

#### *Statistics*

All data analyses were performed using R version 3.5.1. Microbiome community diversity was calculated as the rarefied richness of observed OTUs, which have more than 10 reads. Changes in community composition were assessed with a principal component analysis (PCA) by using the function 'prcomp' in R package 'vegan', and PCA was visualized by using function 'autoplot' in R package 'ggfortify', function adonis in R package 'vegan' was conducted to evaluate the significant difference in community structure across the different growth stages. Community-level FD was calculated based on quantitative carbon utilization metrics of the co-occurring isolates with R package 'picante'. Briefly, a distance matrix was computed based on quantitative resource utilization metrics by function dist. Then a neighbor-joining tree was

drawn based on the distance matrix by function 'nj'. FD was subsequently calculated as the sum of the total phylogenetic branch length in the neighbor-joining phylogenetic tree for the community by function 'pd'. The effects of plant growth stages on rhizosphere microbiome FD, bacterial growth in reduced nutrient availability, bacterial supernatant pathogen suppression ability and microbiome community level pathogen suppression ability were computed using a linear model, with plant development stages as factors. Then, statistical analyses were conducted with Tukey multiple comparison tests in R by using function 'TukeyHSD' after converting the linear model object with function 'aov'. For assessing which characteristic could better predict the microbiome community level pathogen suppressiveness, we used a linear model to predict the effect of carbon use-based FD, growth stability under stress and pathogen antagonistic activity on the invasibility of re-assembled consortia.

### Acknowledgements

We thank Jing Ma and Shaohua Gu for assisting with the experiments. This research was financially supported by the National Key Research and Development Program of China (2018YFD1000800), the Fundamental Research Funds for the Central Universities (grant numbers KJYQ202002, KYGD202006), the National Natural Science Foundation of China (31972504 to Y.X. and 41922053 to Z.W.). A.J. and J.H. are supported by the NWO grant ALW.870.15.050 and the TKI top-sector grant KV1605 082. J.H. is supported by the Chinese Scholarship Council (CSC) joint PhD scholarship (grant 201506850027).

### References

- Achouak, W., Conrod, S., Cohen, V., and Heulin, T. (2004) Phenotypic variation of *Pseudomonas brassicacearum* as a plant root-colonization strategy. *Mol Plant Microbe Interact* **17**: 872–879.
- Amato, K.R., Yeoman, C.J., Kent, A., Righini, N., Carbonero, F., Estrada, A., et al. (2013) Habitat degradation impacts black howler monkey (*Alouatta pigra*) gastrointestinal microbiomes. *ISME J* **7**: 1344–1353.
- Barret, M., Morrissey, J.P., and O'Gara, F. (2011) Functional genomics analysis of plant growth-promoting rhizobacterial traits involved in rhizosphere competence. *Biol Fertil Soils* **47**: 729–743.
- Beckers, B., Op De Beeck, M., Weyens, N., Boerjan, W., and Vangronsveld, J. (2017) Structural variability and niche differentiation in the rhizosphere and endosphere bacterial microbiome of field-grown poplar trees. *Microbiome* **5**: 25.
- Bordelon, H., Russ, P.K., Wright, D.W., and Haselton, F.R. (2013) A magnetic bead-based method for concentrating DNA from human urine for downstream detection. *PLoS One* **8**: e68369.
- Cadotte, M.W., Carscadden, K., and Mirotchnick, N. (2011) Beyond species: functional diversity and the maintenance of ecological processes and services. *J Appl Ecol* **48**: 1079–1087.
- Cardenas, E., Wu, W.-M., Leigh, M.B., Carley, J., Carroll, S., Gentry, T., et al. (2010) Significant association between sulfate-reducing bacteria and uranium-reducing microbial communities as revealed by a combined massively parallel sequencing-indicator species approach. *Appl Environ Microbiol* **76**: 6778–6786.
- Chaparro, J.M., Badri, D.V., and Vivanco, J.M. (2014) Rhizosphere microbiome assemblage is affected by plant development. *ISME J* **8**: 790–803.
- Dang, H., and Lovell, C.R. (2000) Bacterial primary colonization and early succession on surfaces in marine waters as determined by amplified rRNA gene restriction analysis and sequence analysis of 16S rRNA genes. *Appl Environ Microbiol* **66**: 467–475.
- Díaz, S., Fargione, J., Chapin, F.S., and Tilman, D. (2006) Biodiversity loss threatens human well-being. *PLoS Biol* **4**: e277.
- Dimitrakopoulos, P.G., and Schmid, B. (2004) Biodiversity effects increase linearly with biotope space. *Ecol Lett* **7**: 574–583.
- Dinesh, R., Anandaraj, M., Kumar, A., Bini, Y.K., Subila, K. P., and Aravind, R. (2015) Isolation, characterization, and evaluation of multi-trait plant growth promoting rhizobacteria for their growth promoting and disease suppressing effects on ginger. *Microbiol Res* **173**: 34–43.
- Dini-Andreote, F., Stegen, J.C., van Elsas, J.D., and Salles, J.F. (2015) Disentangling mechanisms that mediate the balance between stochastic and deterministic processes in microbial succession. *Proc Natl Acad Sci U S A* **112**: E1326–E1332.
- Edgar, R.C. (2013) UPARSE: highly accurate OTU sequences from microbial amplicon reads. *Nat Methods* **10**: 996–998.
- Fargione, J.E., and Tilman, D. (2005) Diversity decreases invasion via both sampling and complementarity effects. *Ecol Lett* **8**: 604–611.
- Garcia, J., and Kao-Kniffin, J. (2018) Microbial group dynamics in plant rhizospheres and their implications on nutrient cycling. *Front Microbiol* **9**: 1516.
- Haas, D., and Défago, G. (2005) Biological control of soil-borne pathogens by fluorescent *pseudomonads*. *Nat Rev Microbiol* **3**: 307–319.
- Helsen, K., Hermy, M., and Honnay, O. (2016) A test of priority effect persistence in semi-natural grasslands through the removal of plant functional groups during community assembly. *BMC Ecol* **16**: 22.
- Heuer, H., Krsek, M., Baker, P., Smalla, K., and Wellington, E.M.H. (1997) Analysis of Actinomycete communities by specific amplification of genes encoding 16S rRNA and gel-electrophoretic separation in denaturing gradients. *Appl Environ Microbiol* **63**: 9.
- Hu, J., Wei, Z., Friman, V.-P., Gu, S., Wang, X., Eisenhauer, N., et al. (2016) Probiotic diversity enhances rhizosphere microbiome function and plant disease suppression. *mBio* **7**: e01790–e01716.
- Jeraldo, P., Sipos, M., Chia, N., Brulc, J.M., Dhillon, A.S., Konkel, M.E., et al. (2012) Quantification of the relative roles of niche and neutral processes in structuring gastrointestinal microbiomes. *Proc Natl Acad Sci U S A* **109**: 9692–9698.

- Jiang, G., Wei, Z., Xu, J., Chen, H., Zhang, Y., She, X., *et al.* (2017) Bacterial wilt in china: history, current status, and future perspectives. *Front Plant Sci* **8**: 1549.
- Jousset, A., Bienhold, C., Chatzinotas, A., Gallien, L., Gobet, A., Kurm, V., *et al.* (2017) Where less may be more: how the rare biosphere pulls ecosystems strings. *ISME J* **11**: 853–862.
- Jousset, A., Schmid, B., Scheu, S., and Eisenhauer, N. (2011a) Genotypic richness and dissimilarity opposingly affect ecosystem functioning. *Ecol Lett* **14**: 537–545.
- Jousset, A., Schulz, W., Scheu, S., and Eisenhauer, N. (2011b) Intraspecific genotypic richness and relatedness predict the invasibility of microbial communities. *ISME J* **5**: 1108–1114.
- Kährström, C.T. (2014) Bacterial pathogenesis: Bacteria choose to fight and flee. *Nat Rev Microbiol* **12**: 460–461.
- Koenig, J.E., Spor, A., Scalfone, N., Fricker, A.D., Stombaugh, J., Knight, R., *et al.* (2011) Succession of microbial consortia in the developing infant gut microbiome. *Proc Natl Acad Sci U S A* **108**: 4578–4585.
- Li, M., Wei, Z., Wang, J., Jousset, A., Friman, V.-P., Xu, Y., *et al.* (2019) Facilitation promotes invasions in plant-associated microbial communities. *Ecol Lett* **22**: 149–158.
- Lugtenberg, B., and Kamilova, F. (2009) Plant-growth-promoting rhizobacteria. *Annu Rev Microbiol* **63**: 541–556.
- Lundberg, D.S., Lebeis, S.L., Paredes, S.H., Yourstone, S., Gehring, J., Malfatti, S., *et al.* (2012) Defining the core *Arabidopsis thaliana* root microbiome. *Nature* **488**: 86–90.
- Margesin, R., Płaza, G.A., and Kasenbacher, S. (2011) Characterization of bacterial communities at heavy-metal-contaminated sites. *Chemosphere* **82**: 1583–1588.
- Marilley, L., and Aragno, M. (1999) Phylogenetic diversity of bacterial communities differing in degree of proximity of *Lolium perenne* and *Trifolium repens* roots. *Appl Soil Ecol* **13**: 127–136.
- Mendes, L.W., Kuramae, E.E., Navarrete, A.A., van Veen, J. A., and Tsai, S.M. (2014) Taxonomical and functional microbial community selection in soybean rhizosphere. *ISME J* **8**: 1577–1587.
- Mendes, R., Kruijt, M., de Bruijn, I., Dekkers, E., van der Voort, M., Schneider, J.H.M., *et al.* (2011) Deciphering the rhizosphere microbiome for disease-suppressive bacteria. *Science* **332**: 1097–1100.
- Molina, L. (2000) Survival of *Pseudomonas putida* KT2440 in soil and in the rhizosphere of plants under greenhouse and environmental conditions. *Soil Biol Biochem* **32**: 315–321.
- Morgan, J.A.W., Bending, G.D., and White, P.J. (2005) Biological costs and benefits to plant–microbe interactions in the rhizosphere. *J Exp Bot* **56**: 1729–1739.
- Pérez-Jaramillo, J.E., Carrión, V.J., de Hollander, M., and Raaijmakers, J.M. (2018) The wild side of plant microbiomes. *Microbiome* **6**: 143.
- Pickett, S.T.A., and McDonnell, M.J. (1989) Changing perspectives in community dynamics: a theory of successional forces. *Trends Ecol Evol* **4**: 241–245.
- Saleem, M., Hu, J., and Jousset, A. (2019) More than the sum of its parts: microbiome biodiversity as a driver of plant growth and soil health. *Annu Rev Ecol Evol Syst* **50**: 145–168.
- Schnider-Keel, U., Seematter, A., Maurhofer, M., Blumer, C., Duffy, B., Gigot-Bonnefoy, C., *et al.* (2000) Autoinduction of 2,4-diacetylphloroglucinol biosynthesis in the biocontrol agent *Pseudomonas fluorescens* CHA0 and repression by the bacterial metabolites salicylate and pyoluteorin. *J Bacteriol* **182**: 1215–1225.
- Shi, S., Nuccio, E.E., Shi, Z.J., He, Z., Zhou, J., and Firestone, M.K. (2016) The interconnected rhizosphere: High network complexity dominates rhizosphere assemblages. *Ecol Lett* **19**: 926–936.
- Smalla, K., Wieland, G., Buchner, A., Zock, A., Parzy, J., Kaiser, S., *et al.* (2001) Bulk and rhizosphere soil bacterial communities studied by denaturing gradient gel electrophoresis: plant-dependent enrichment and seasonal shifts revealed. *Appl Environ Microbiol* **67**: 4742–4751.
- Smead, R., and Forber, P. (2013) The evolutionary dynamics of spite in finite populations. *Evolution* **67**: 698–707.
- Stegen, J.C., Lin, X., Konopka, A.E., and Fredrickson, J.K. (2012) Stochastic and deterministic assembly processes in subsurface microbial communities. *ISME J* **6**: 1653–1664.
- Tilman, D. (1987) Secondary succession and the pattern of plant dominance along experimental nitrogen gradients. *Ecol Monogr* **57**: 189–214.
- Voelkerding, K.V., Dames, S.A., and Durtschi, J.D. (2009) Next-generation sequencing: from basic research to diagnostics. *Clin Chem* **55**: 641–658.
- Wei, Z., Yang, T., Friman, V.-P., Xu, Y., Shen, Q., and Jousset, A. (2015) Trophic network architecture of root-associated bacterial communities determines pathogen invasion and plant health. *Nat Commun* **6**: 8413.
- Wei, Z., Yang, X., Yin, S., Shen, Q., Ran, W., and Xu, Y. (2011) Efficacy of *Bacillus*-fortified organic fertiliser in controlling bacterial wilt of tomato in the field. *Appl Soil Ecol* **48**: 152–159.
- Weller, D.M., Raaijmakers, J.M., Gardener, B.B.M., and Thomashow, L.S. (2002) Microbial populations responsible for specific soil suppressiveness to plant pathogens. *Annu Rev Phytopathol* **40**: 309–348.
- Whittaker, R.J. (1993) Plant population patterns in a glacier foreland succession: pioneer herbs and later-colonizing shrubs. *Ecography* **16**: 117–136.
- Yarwood, S.A., Bottomley, P.J., and Myrold, D.D. (2010) Soil microbial communities associated with douglas-fir and red alder stands at high- and low-productivity forest sites in Oregon, USA. *Microb Ecol* **60**: 606–617.

## Supporting Information

Additional Supporting Information may be found in the online version of this article at the publisher's web-site:

**Fig. S1.** Carbon resource utilization patterns of each individual bacterium isolated from different growth stage tomato rhizosphere. Y-axis are the names of different carbon resources; x-axis are genus names of each isolated bacterium. Panel A: carbon resource utilization pattern of bacteria isolated from bulk soil; Panel B: carbon resource utilization pattern of bacteria isolated from rhizosphere at seedling stage; Panel C: carbon resource utilization pattern of bacteria isolated from rhizosphere at flowering stage; Panel D: carbon resource utilization pattern of bacteria isolated from rhizosphere at fruiting

stage. The filled square represents that the bacterium on the x-axis is able to use the carbon on the y-axis. The empty square represents that the bacterium on the x-axis is not able to use the carbon on the y-axis

**Fig. S2.** Coefficients of variation for bacterial growth ability under each stressor reduced nutrient availability (10x reduction in culture medium concentration), oxidative stress (1 mM H<sub>2</sub>O<sub>2</sub>) or high salinity (200 mM NaCl). One point corresponds to one sample, coefficients of variation was calculated for all the 32 isolates from each sample. A higher coefficient of variation indicates the co-occurrence of a wider

range of life history strategies with respect to stress tolerance.

**Fig. S3.** Inhibitory activity of supernatants from different phylogenetic orders of bacteria isolated from different growth stage tomato rhizosphere. Each point shows one bacterial isolate.

**Table S1.** Information about bacterial isolates at phylum, order and genus level.

**Table S2.** Carbon resources used to quantify community level functional diversity.

**Table S3.** Supplementary Table